04

Crystal structure and cationic ordering in ludwigites $Co_{3-x}Ni_xBO_5$

© S.N. Sofronova, A.V. Chernyshev, A.D. Vasiliev, A.V. Shabanov

Kirensky Institute of Physics SB RAS —
standalone subdivision of the Federal Research Center „Krasnoyarsk Scientific Center of SB RAS“,
Krasnoyarsk, Russia

E-mail: ssn@iph.krasn.ru

Received September 17, 2024
Revised September 17, 2024
Accepted September 28, 2024

The structure and composition of two solid solutions of $Co_{3-x}Ni_xBO_5$ with the ludwigite structure, the nickel ion concentrations in which are $x = 0.33$ and $x = 0.59$, are determined. Within the framework of the first-principles calculation, the cationic ordering for three concentrations $x = 0.25, 0.5, 0.75$. It was found that nickel cations prefer to occupy positions 2a and 4g.

Keywords: ludwigite, cation ordering, crystal structure.

DOI: 10.61011/PSS.2024.10.59627.240

1. Introduction

Transition metal borates are of interest because they can be realized in various structural types. There are known compounds $Mn_3B_2O_6$, $Co_3B_2O_6$ with a kotoite structure [1,2], Mn_3BO_5, Co_3BO_5 with ludwigite structure [3,4] and Mn_2BO_4 with the structure of warwickite [5], manganese tetraborate MnB_4O_7 [6] and others [7]. Depending on the crystallization conditions, one or another structural type of borates can occur, which, in turn, significantly affects the properties of compounds. So, cobalt ions enter only in the divalent state in $Co_3B_2O_6$ with a kotoite structure, a transition to the antiferromagnetic state is observed in the compound [8]. Cobalt ions are present in trivalent and divalent states in ludwigite Co_3BO_5, with trivalent ions in a low spin state with spin 0, and the magnetic ordering is ferrimagnetic [9].

It is known about the existence of solid solutions of $Co_{3-x}Ni_xBO_5$ with a kotoite structure [1,6,10–12], however, solid solutions of $Co_{3-x}Ni_xBO_5$ with ludwigite structure are not currently studied. The spin state of cobalt ions can change from low spin (at high concentrations) to high spin in $Co_{3-x}Ni_xBO_5$ compounds, depending on the concentration (at concentrations x, close to 1). In addition, many ludwigites are characterized by the division of the magnetic system into two magnetic subsystems with a non-collinear orientation of the magnetic moments of the subsystems [13–17]. The division into two magnetic subsystems may also occur in solid solutions of $Co_{3-x}Ni_xBO_5$ if trivalent cobalt ions are in a high spin state. Substitution of cobalt ions with nickel ions in the divalent subsystem and obtaining of crystals $Co^{3+}Ni^{2+}_{2-x}Co^{2+}_xBO_5$ with ludwigite structure is an interesting growth problem that was first solved by us in the previous study [12]. Our studies showed that it is necessary to control the valence of cobalt cations for obtaining $Co^{3+}Ni^{2+}_{2-x}Co^{2+}_xBO_5$ crystals with a ludwigite structure from melt solutions. A change of the valence of cobalt from 3+ to 2+ results in the growth of borates with a graphite structure in which metal ions are present only in the divalent state. It was shown in Ref. [12] that compounds crystallized into a phase with a ludwigite structure at low concentrations of nickel ions in the solution-melt system; the crystallization phase was a phase with a kotoite structure with an increase of the concentration of nickel ions. We present in this paper a study of the compositions, crystal structure and cationic ordering of compounds $Co^{3+}Ni^{2+}_{2-x}Co^{2+}_xBO_5$ with the ludwigite structure obtained in the study [12].

2. Composition and crystal structure

Two compositions $Co^{3+}Ni^{2+}_{2-x}Co^{2+}_xBO_5$ with ludwigite structure were obtained by spontaneous generation from a solution-melt system based on $Bi_2Mo_3O_{12}-B_2O_3$, diluted with alkali metal carbonates Na_2CO_3 [12]. The synthesized crystals are have a black color with a needle-like shape (Figure 1). The obtained single crystals were studied using the TM-4000Plus tabletop scanning election microscope by Hitachi at an accelerating voltage of 20 kV. Element mapping was carried out using Bruker XFlash 630Hc X-ray detector. Spectra were analyzed using Quantax70 software. All samples had uniform compositions. The spectra of different crystal sites for all groups of samples were compared to check the uniformity.

Images of crystals are shown in Figure 1. The ratios of nickel and cobalt ions, determined using the scanning microscopy method, and the chemical formulas of the compounds for the two compositions are given in Table 1, the ratios of transition metal ions in the melt-solution are also indicated there.

It can be seen from the table that there is a qualitative agreement between the content of ions in the „flux“ and the actual content of nickel and cobalt in the compounds.

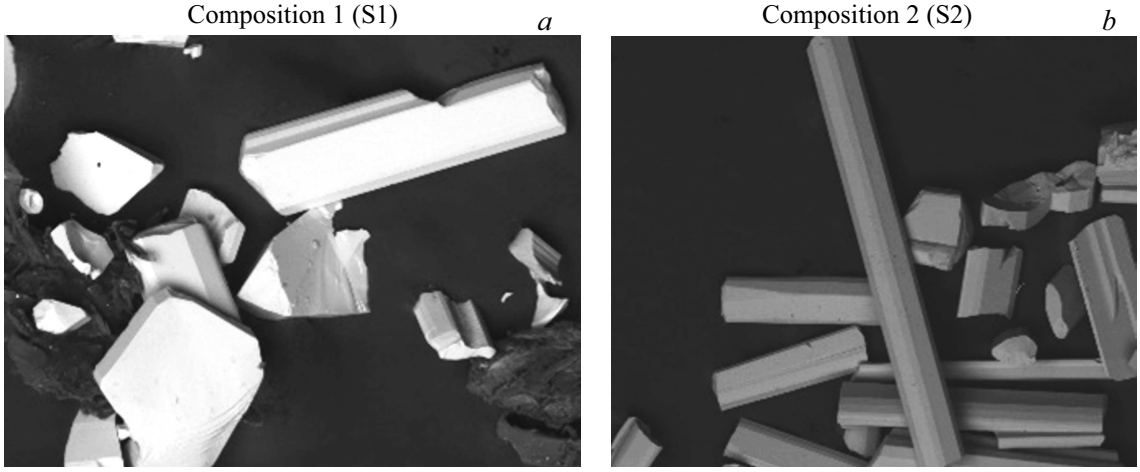

Figure 1. Photos of samples of solid solutions of $Co_{3-x}Ni_xBO_5$ obtained using a desktop scanning electron microscope: *a*) composition S1, *b*) composition S2.

Table 1. Comparison of the actual composition of the obtained samples and the composition of „flux" for each sample

Composition	Ratio of Ni : Co		Chemical formula
	in solution-melt	in crystal	
S1	1 : 11	1 : 8,1	$Co^{3+}Ni^{2+}_{0.33}Co^{2+}_{1.67}BO_5$
S2	1 : 11	1 : 4,1	$Co^{3+}Ni^{2+}_{0.59}Co^{2+}_{1.41}BO_5$

However, the actual nickel content exceeds the nickel content in the melt solution, which emphasizes the difference in the distribution coefficients of cobalt and nickel oxides in the used melt solutions — the lower solubility of nickel oxide results in a greater presence of this element in the crystal [12].

3. Crystal structure and cationic ordering

The crystal structure was studied on single crystal samples by X-ray diffraction using SMART APEXII diffractometer (MoK_α, $\lambda = 0.7106$ Å). The space group, the parameters of the crystal lattice for compositions S1 and S2 are listed in Table 2, and coordinates of atoms for composition S1 are listed in Table 3.

The coordinates of the atoms for the composition of S2 were not specified, since the change in the parameters of the crystal lattice relative to the composition of S1 is less than one percent, it is unlikely that there will be a significant change in the coordinates of the atoms in the crystal lattice. The distances between ions for the composition S1 are provided in Table A1 of the Appendix, the distances $Me-O$ are also indicated below for clarity when comparing different compositions with the ludwigite structure. The metallic ions Co and Ni are indicated in the table as Me, since it is impossible to distinguish nickel and cobalt ions using the X-ray diffraction method, therefore, it is impossible to determine the population of crystallographic positions.

As we noted earlier, metal ions in compositions with the ludwigite structure $(Me, Me')_3BO_5$ should have different valence according to the condition of electroneutrality. In

Table 2. Parameters of the crystal lattice of compositions S1 and S2. Space group $Pbam$ in both cases (55)

Composition		S1	S2
V, Å^3		332.96(4)	333.76(5)
R-factor		0.032	0.036
Parameters of cells, Å	*a*	9.2855(7)	9.244(5)
	b	11.9893(9)	12.049(5)
	c	2.9908(2)	2.9966(14)

Table 3. Atomic coordinates $Co^{3+}Ni^{2+}_{0.33}Co^{2+}_{1.67}BO_5$ (composition 1). U^*_{iso} — isotropic, U_{eq} — equivalent isotropic displacement parameters

Atom	Position	Coordinates of atoms			U^*_{iso}/U_{eq}
		x/a	y/b	z/c	
Me_1	2a	1/2	1/2	0	0.00631(12)
Me_2	2d	0	1/2	1/2	0.00589(12)
Me_3	4g	0.49645(3)	0.77727(3)	0	0.00627(10)
O_1	4g	0.8797(2)	0.57741(17)	0	0.0123(3)
O_2	4h	0.83880(18)	0.76125(16)	1/2	0.0083(3)
O_3	4h	0.65673(19)	0.45974(15)	1/2	0.0087(3)
O_4	4g	0.6133(2)	0.64255(14)	0	0.0091(3)
O_5	4h	0.8821(2)	0.36128(14)	1/2	0.0083(3)
B	4h	0.7346(3)	0.3618(2)	1/2	0.0065(4)

Table 4. Calculated differences of energies ΔE of various cationically ordered configurations with respect to the lowest energy configuration for the composition $Co^{3+}Ni^{2+}_{0.25}Co^{2+}_{1.75}BO_5$

Ion №	№ of cationically ordered state												ΔE
	2a		2d		4g				4h				
	1	2	3	4	5	6	7	8	9	10	11	12	
1	Ni	Co	Co	Co	Co	Co	Co	Co	Co	Co	Co	Co	0.031396
2	Co	Ni	Co	Co	Co	Co	Co	Co	Co	Co	Co	Co	0.028042
3	Co	Co	Co	Co	Ni	Co	Co	Co	Co	Co	Co	Co	0
4	Co	Co	Co	Co	Co	Co	Co	Co	Ni	Co	Co	Co	0.026700

Table 5. Calculated energy differences ΔE of various cationically ordered configurations with respect to the lowest energy configuration for the composition $Co^{3+}Ni^{2+}_{0.5}Co^{2+}_{1.5}BO_5$

Ion №	№ of cationically ordered state												ΔE
	2a		2d		4g				4h				
	1	2	3	4	5	6	7	8	9	10	11	12	
1	Ni	Ni	Co	Co	Co	Co	Co	Co	Co	Co	Co	Co	0.021299
2	Co	Co	Ni	Ni	Co	Co	Co	Co	Co	Co	Co	Co	0.017804
3	Co	Co	Co	Co	Ni	Ni	Co	Co	Co	Co	Co	Co	0.078141
4	Co	Co	Co	Co	Co	Co	Co	Co	Ni	Ni	Co	Co	0.021322
5	Co	Ni	Ni	Co	Co	Co	Co	Co	Co	Co	Co	Co	0.0174404
6	Ni	Co	Co	Co	Ni	Co	Co	Co	Co	Co	Co	Co	0
7	Co	Ni	Co	Co	Co	Co	Co	Co	Ni	Co	Co	Co	0.017698
8	Co	Ni	Co	Co	Ni	Co	Co	Co	Co	Co	Co	Co	0.01675

Table 6. Calculated energy differences of various cationically ordered configurations with respect to the lowest energy configuration for the composition $Co^{3+}Ni^{2+}_{0.75}Co^{2+}_{1.25}BO_5$

Ion №	№ of cationically ordered state												ΔE
	2a		2d		4g				4h				
	1	2	3	4	5	6	7	8	9	10	11	12	
1	Ni	Ni	Co	Co	Ni	Co	Co	Co	Co	Co	Co	Co	0
2	Ni	Co	Co	Co	Ni	Ni	Co	Co	Co	Co	Co	Co	0.037859
3	Co	Ni	Co	Co	Ni	Ni	Co	Co	Co	Co	Co	Co	0.036366
4	Co	Ni	Co	Co	Co	Co	Ni	Ni	Co	Co	Co	Co	0.000383
5	Co	Ni	Co	Co	Co	Ni	Ni	Co	Co	Co	Co	Co	0.032364
6	Ni	Co	Co	Co	Co	Ni	Ni	Co	Co	Co	Co	Co	0.032362
7	Co	Ni	Co	Co	Ni	Co	Co	Ni	Co	Co	Co	Co	0.032373

Table 7. Distances d_{Me-O} for each crystallographic position for compounds Ni_2GaBO_5 [24], Ni_2AlBO_5 [24], Co_3BO_5 [3] and $Co^{3+}Ni^{2+}_{0.33}Co^{2+}_{1.67}BO_5$ and the ionic radius of the trivalent ion $r_{Me^{3+}}$. Indicated for all bonds

Composition	Crystallographic Position	2a	2d	4g	4h	$r_{Me^{3+}}$, nm
Ni_2GaBO_5	d_{Me-O}, AA/number of bonds	2.004/2 2.094/4	2.038/2 2.061/4	1.948 2.015 2.102/2 2.105/2	2.052 2.065 1.942/2 2.067/2	0.063 (Ga^{3+})
	$\langle d_{Me-O}\rangle$, Å	2.064	2.053	2.062	2.022	
	Occupancy, % for Ni^{2+}	100.0	100.0	100.0	0	
Ni_2AlBO_5	d_{Me-O}, AA/number of bonds	1.972/2 2.070/4	1.97/2 2.012/4	1.96 2.054 2.093/2 2.103/2	1.99 2.01 1.89/2 2.045/2	0.052 (Al^{3+})
	$\langle d_{Me-O}\rangle$, Å	2.037	1.998	2.067	1.978	
	Occupancy, % for Ni^{2+}	65.2	89.0	85.2	35.8	
Co_3BO_5	d_{Me-O}, AA/number of bonds	1.998/2 2.142/4	1.988/2 2.101/4	1.944 2.047 2.113/2 2.135/2	1.97 1.98 1.920/2 1.978/2	0.055 (Co^{3+}, in low spin state)
	$\langle d_{Me-O}\rangle$, Å	2.094	2.063	2.081	1.957	
	Occupancy, % for Co^{2+}	100.0	100.0	100.0	0.0	
$Co^{3+}Ni^{2+}_{0.33}Co^{2+}_{1.67}BO_5$	d_{Me-O}, AA/number of bonds	2.007/2 2.141/4	1.991/2 2.084/4	1.946 2.052 2.126/2 2.143/2	1.993 2.000 1.943/2 2.017/2	? (not known confidently)
	$\langle d_{Me-O}\rangle$, Å	2.096	2.053	2.089	1.985	
	Estimated occupancy, % for Me^{2+}	100.0	100.0	100.0	0.0	

our case, cobalt ions are trivalent ions in compounds $Co_{3-x}Ni_xBO_5$, nickel ions are part of ludwigites in the divalent state. To correctly describe the magnetic properties, it is necessary to know the distribution of magnetic ions in crystallographic positions. The neutron diffraction method is a direct experimental method which can determine the distribution of ions over positions. In addition to the fact that this method is not widely available, it is very difficult to study of borates using the neutron diffraction method because of the high absorption capacity of boron ions. *ab initio* calculations can be used to model the distribution of metal ions over positions. The energies of various cationically ordered configurations can be compared using *ab initio* approaches, determining which distribution of cations by positions is the most advantageous.

The ludwigite unit cell contains 12 transition metal ions, which occupy four crystallographic positions: 2a, 2d, 4g and 4h. The ludwigite structure is shown in Figure 2.

Using the Wien2K software package, we calculated the total energies of various cationically ordered configurations for three compositions: $Co^{3+}Ni^{2+}_{0.25}Co^{2+}_{1.75}BO_5$,

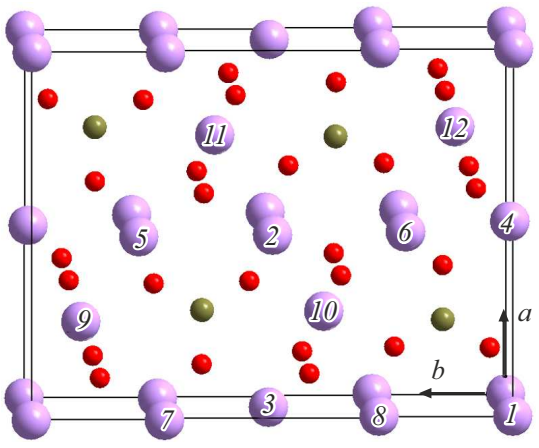

Figure 2. Ludwigite structure. Transition metal ions are indicated by the largest circles and numbered with numbers from *1* to *12*. The ions *1* and *2* occupy the position 2a, the ions *3* and *4* occupy the position 2d, ions *5*–*8* occupy the position 4g, and ions *9*–*12* occupy the position 4h.

$Co^{3+}Ni^{2+}_{0.5}Co^{2+}_{1.5}BO_5$, $Co^{3+}Ni^{2+}_{0.75}Co^{2+}_{1.25}BO_5$. One cobalt ion is replaced by a nickel ion in the first composition, two cobalt ions are replaced by nickel ions in the second composition, and three cobalt ions are replaced by nickel ions in the third composition.

The Wien2K software package uses the method of linearized coupled plane waves with local orbitals [18,19]. The exchange-correlation energy is calculated in the least squares approximation (LSDA) [20] taking into account the density gradient [21], the Hubbard correlation coefficients are also taken into account. We used the potentials $U = 0.52$ Ry and $J = 0$ Ry [22] for transition metal ions in the calculation. A set of 400 k points in the Brillouin zone was used for finding the total energy. Value $R_{MT}K_{max} = 6.0$ (R_{MT} — minimum radius of MT spheres, K_{max} —plane wave cutoff vector). The accuracy of the energy calculation was 1 μRy. The following radii of atomic spheres were used in the calculations: 1.91 atomic units for nickel ions, 1.86 at.u. for cobalt ions, 1.13 at.u. for boron ions and 1.31 at.u. for oxygen. The modified Blehl tetrahedron method was used to calculate the total density of states [23].

Tables 4–6 shows the calculated energy differences of various cationically ordered configurations with respect to the configuration with the lowest energy.

Nickel ions primarily replace cobalt ions in positions 4g and 2a as can be seen from Tables 4–6. According to the data obtained by neutron diffraction in ludwigite Co_3BO_5, positions 2a, 2d, 4g are occupied by divalent cobalt ions, and position 4h are occupied by trivalent cobalt ions in the low spin state [9]. The ionic radii of divalent cobalt and nickel ions are close to $r^{2+}_{Co} = 0.074$ nm and $r^{2+}_{Ni} = 0.072$ nm. Whereas the ionic radii of trivalent cobalt ions are significantly smaller: in the high-spin state $r^{3+}_{Co} = 0.061$ nm, and in the low-spin state $r^{3+}_{Co} = 0.055$ nm.

The distances Me–O, as well as the populations of divalent cations for each crystallographic position for four compounds Ni_2GaBO_5, Ni_2AlBO_5, Co_3BO_5 and $Co^{3+}Ni^{2+}_{0.33}Co^{2+}_{1.67}BO_5$ are listed in Table 7 [3.24].

The positions 2a, 2d, 4g are occupied only by divalent nickel and cobalt ions, respectively, in compounds Ni_2GaBO_5 and Co_3BO_5. It can be seen in Table 7 that the average distances Me–O for positions 2a, 2d, 4g in these bonds differ by less than 1.5%, whereas for position 4h the difference is 3.5%. The ionic radius of gallium is greater than the ionic radius of trivalent cobalt in the low spin state, the average bond length is Ga–O more than Co–O. The trivalent ion has the smallest ionic radius in the Ni_2AlBO_5 compound, the trivalent ion is present in this compound with different concentrations in all crystallographic positions, it can be seen that the average length of bond Me–O for position 2d is less than for other compositions in Table 7. Substitution of cobalt ions for nickel ions in the compound $Co^{3+}Ni^{2+}_{0.33}Co^{2+}_{1.67}BO_5$ changes the lengths of bonds Me–O within 1–2% with respect to Co_3BO_5, the average length of bond Me–O varies within the same limits, in particular, for position 4h, which allows assuming that nickel ions replace cobalt ions in the divalent state in positions 2a, 2d, 4g.

4. Conclusion

The composition of the two subject solid solutions: $Co^{3+}Ni^{2+}_{0.33}Co^{2+}_{1.67}BO_5$ and $Co^{3+}Ni^{2+}_{0.59}Co^{2+}_{1.41}BO_5$ was studied using scanning microscopy, the crystal structure, lattice parameters and atomic coordinates were determined. *ab initio* calculation of energies of various cationically ordered configurations showed that nickel ions prefer to replace cobalt ions at positions 2a and 4g, which is qualitatively consistent with experimental data.

Acknowledgments

The research was carried out using the equipment provided by the Krasnoyarsk Regional Center for Collective Use.

The authors would like to thank E.M. Moshkina for the samples provided for the study.

Funding

The study was carried out with the support of the Russian Science Foundation and Krasnoyarsk Regional Fund for the Support of Scientific and Scientific-technical activities, project no. 23-12-20012 (https://rscf.ru/project/23-12-20012/).

Conflict of interest

The authors declare that they have no conflict of interest.

Appendix

Symmetry Codes:

(i) $x, y, z-1$; (ii) $x+1, y, z$;

(iii) $x, y, z+1$; (iv) $-x+1, -y+1, -z$;

(v) $x-1, y, z$; (vi) $-x+1, -y+1, -z+1$;

(vii) $x-1, y, z-1$; (viii) $x-1/2, -y+3/2, z$;

(ix) $-x+3/2, y+1/2, -z+1$;

(x) $-x+3/2, y+1/2, -z$;

(xi) $x-1/2, -y+3/2, z+1$; (xii) $x+1/2, -y+3/2, z$;

(xiii) $x+1, y, z+1$; (xiv) $x+1/2, -y+3/2, z-1$;

(xv) $-x+3/2, y-1/2, -z+1$;

(xvi) $-x+3/2, y-1/2, -z$.

Table A1. Distances between atoms in compound $Co^{3+}Ni^{2+}_{0.33}Co^{2+}_{1.67}BO_5$

d (Me–O), Å		d (Me–Me), Å		d (B–O), Å	
$Co_1–O_4$	2.0067(17)	$Co_1–Co_1^{i}$	2.9908(2)	$B–O_3$	1.379(3)
$Co_1–O_4^{vi}$	2.0068(17)	$Co_1–Co_1^{iii}$	2.9908(2)	$B–O_5$	1.370(3)
$Co_1–O_3$	2.1418(13)			$B–O_2^{xvi}$	1.385(3)
$Co_1–O_3^{iv}$	2.1418(13)				
$Co_1–O_3^{iii}$	2.1418(13)				
$Co_1–O_3^{vi}$	2.1418(13)				
$Co_2–O_5^{iv}$	1.9910(17)	$Co_2–Co_4^{v}$	2.7566(3)	–	–
$Co_2–O_5^{v}$	1.9910(17)	$Co_2–Co_4^{iv}$	2.7566(3)		
$Co_2–O_1^{vi}$	2.0847(13)	$Co_2–Co_2^{iii}$	2.9908(2)		
$Co_2–O_1^{vii}$	2.0847(13)	$Co_2–Co_2^{i}$	2.9908(2)		
$Co_2–O_2^{iv}$	2.0847(13)				
$Co_2–O_1^{v}$	2.0847(13)				
$Co_3–O_4$	1.9456(18)	$Co_3–Co_3^{iii}$	2.9908(2)	–	–
$Co_3–O_1^{viii}$	2.052(2)	$Co_3–Co_3^{i}$	2.9908(2)		
$Co_3–O_5^{ix}$	2.1265(13)				
$Co_3–O_5^{x}$	2.1265(13)				
$Co_3–O_2^{viii}$	2.1430(12)				
$Co_3–O_2^{xi}$	2.1430(12)				
$Co_4–O_4^{i}$	1.9431(12)	$Co_4–Co_2^{ii}$	2.7566(3)	–	–
$Co_4–O_4$	1.9431(12)	$Co_4–Co_4^{i}$	2.9908(2)		
$Co_4–O_3$	1.9930(19)	$Co_4–Co_4^{iii}$	2.9908(2)		
$Co_4–O_2$	1.9998(19)				
$Co_4–O_1$	2.0170(13)				
$Co_4–O_1^{i}$	2.0170(13)				

References

[1] R.E. Newnham, R.P. Santoro, P.F. Seal, G.R. Stallings. Physica Status Solidi (b) **16**, *1*, K17 (1966).
[2] H. Effenberger, F. Pertlik. Z. Kristallographie **166**, *1–4*, 129 (1984).
[3] A. Utzolino, K. Bluhm. Z. Naturforsch. **51b**, 1433 (1996).
[4] R. Norrestam, K. Nielsen, I. Søtofte, N. Thorup. Z. Kristallographie **189**, *1–4*, 33 (1989).
[5] R. Norrestam, M. Kritikos, A. Sjödin. J. Solid State Chem. **114**, *2*, 311 (1995).
[6] S.C. Abrahams, J.L. Bernstein, P. Gibart, M. Robbins, R.C. Sherwood. J. Chem. Phys. **60**, *5*, 1899 (1974).
[7] R.S. Bubnova, Y.P. Biryukov, S.K. Filatov. Russ. J. Inorg. Chem. (2024). https://doi.org/10.1134/S0036023623603434
[8] L.N. Bezmaternykh, S.N. Sofronova, N.V. Volkov, E.V. Eremin, O.A. Bayukov, I.I. Nazarenko, D.A. Velikanov. Physica Status Solidi b **249**, *8*, 1628 (2012).
[9] D.C. Freitas, C.P.C. Medrano, D.R. Sanchez, M. Nuñez Regueiro, J.A. Rodríguez-Velamazán, M.A. Continentino. Phys. Rev. B **94**, *17*, 174409 (2016).
[10] B. Tekin, H. Güler. Mater. Chem. Phys. **108**, *1*, 88 (2008).
[11] H. Güler, B. Tekin. Inorg. Mater. **45**, *5*, 538 (2009).
[12] S. Sofronova, E. Moshkina, A. Chernyshev, A. Vasiliev, N.G. Maximov, A. Aleksandrovsky, T. Andryushchenko, A. Shabanov. CrystEngComm **26**, *19*, 2536 (2024).
[13] J.P. Attfield, J.F. Clarke, D.A. Perkins. Physica B: Condens. Matter **180–181**, *Part 2*, 581 (1992).
[14] P. Bordet, E. Suard. Phys. Rev. B **79**, *14*, 144408 (2009).
[15] S.N. Sofronova, E.V. Eremin, E.M. Moshkina, A.V. Selyanina, G.N. Bondarenko, A.V. Shabanov. Phys. Solid State **64**, *11*, 1743 (2022).
[16] S.N. Sofronova, E.V. Eremin, A.A. Veligzhanin, A.V. Chernyshov, A.V. Kartashev, D.A. Velikanov. Phys. Solid State **65**, *2*, 260 (2023).
[17] E. Moshkina, C. Ritter, E. Eremin, S. Sofronova, A. Kartashev, A. Dubrovskiy, L. Bezmaternykh. J. Phys.: Condens. Matter **29**, *24*, 245801 (2017).
[18] K. Schwarz, P. Blaha. In: R. Dronkowski, S. Kikkawa, A. Stein. Handbook of Solid State Chemistry, Theoretical Description, v. 5. Wiley-VCH Verlag, Weinheim, Germany (2017). Ch. 8, p. 227.
[19] P. Blaha, K. Schwarz, F. Tran, R. Laskowski, G.K.H. Madsen, L.D. Marks. J. Chem. Phys. **152**, *7*, 074101 (2020).
[20] J. Perdew, Y. Wang. Phys. Rev. B **45**, *23*, 13244 (1992).
[21] J.P. Perdew, K. Burke, M. Ernzerhof. Phys. Rev. Lett. **77**, *18*, 3865 (1996).
[22] V.I. Anisimov, J. Zaanen, O.K. Andersen. Phys. Rev. B **44**, *3*, 943 (1991).
[23] P.E. Blöchl, O. Jepsen, O.K. Andersen. Phys. Rev. B **49**, *23*, 16223 (1994).
[24] K. Bluhm, H. Müller-Buschbaum. Z. anorg. allg. Chemie **582**, *1*, 15 (1990).

Translated by A.Akhtyamov